STRAIN RATE BEHAVIOUR AND NOTCH SENSITIVITY OF ALUMINIUM 6082-T6 ALLOY UNDER TENSILE LOADS

Saurav SAGAR[1], Nilamber K. SINGH[2], Nityanand S. MAURYA[3]

An experimental investigation on tensile behaviour of Al6082-T6 alloy is carried out at different strain rates (0.0001-0.1s^{-1}) in room temperature 25°C. The alloy is used in high stress applications such as transportation, defence and offshore structures due to high strength with excellent corrosion resistance. It is found that the alloy is positive sensitive to the strain rates and the heat treatment (50-250°C) affects the tensile properties where heating rate 4°C/min and soaking time 1-3 hours are maintained. Notch Sensitivity of the alloy is studied for various notch profiles (C, U and V) on the tensile specimens. Dissipation energy by the alloy is determined for the above loading conditions. Fractography analysis is done and thereafter, the existing material models (Cowper-Symonds and Johnson-Cook) are evaluated based on experimental data.

Keywords: Al6082-T6, strain rate, notch sensitivity, heat treatment and material models.

1. Introduction

The increasing demand of lightweight metallic materials for crashworthy structures such as automobile, airplane and marine, motivated researchers to study the mechanical characteristics of Al-alloys under various loading conditions due to their high strength to density ratio, good ductility and excellent corrosion resistance. The dynamic tensile behaviour of Al7075-T6 alloy is studied by Zhang et al. [1] whereas, the cyclic plastic deformation of the alloy Al7050-T6 is observed by Branco et al. [2]. Prakash et al. [3-4] found positive strain rate (0.0001-1200s^{-1}) sensitivity of Al2014-T6 alloy and negative strain rate (0.0001-1300s^{-1}) sensitivity of Al5052-H32 alloy. High strain rate (1000-3100s^{-1}) tensile behaviour of AA5182 are studied by Deng et al. [5] using electromagnetic driving technique. Tan et al. [6] predicted the tensile (0.001-2900s^{-1}) flow behaviour of Al7050-T7451 alloy using modified Johnson–Cook model. The cryogenic behaviour (biaxial tension) of Al6061 alloy is discussed by Wang et al. [7] whereas, the precipitation and dislocation behaviour of AA7075-T7352 are studied by Tandon et al. [8]. Bobbili et al. [9] addressed the tensile behaviour of

[1] Res. Scholar, National Institute of Technology Patna, India, e-mail: sauravsagar2k9@gmail.com
[2] Assoc. Professor, National Institute of Technology Patna, India, e-mail: nilambersingh@nitp.ac.in
[3] Professor, National Institute of Technology Patna, India, e-mail: nsmaurya@nitp.ac.in

Al7017 alloy at 25-300℃ and 0.01-1500s^{-1} and, the fracture behaviour (mixed-mode loading) of the forged Al7075-T6 alloy is examined by Hashemian et al. [10]. Huang et al. [11] discussed the forming characteristics (-160℃ to 25℃) of 2A14 aluminum alloy under tension (0.00025 to 0.01s^{-1}). Derpeński et al. [12] considered the ductile fracture of notched aluminum alloy EN-AW 2024-T3 specimens at 100-300℃ and, Combaz et al. [13] observed the hole and notch sensitivity of pure aluminium foam. Mondal et al. [14] detected superior ballistic resistance characteristics of AA7055 alloy in under-aged (8 h at 100℃) and peak-aged (8 h at 100℃ and 24 h at 120℃) conditions compared to the over-aged (24 h at 165℃) condition. Thus, in literatures, several authors have studied different grades of aluminium alloys by using different experimental setups, working conditions and manufacturing processes. Therefore, the variations in experimental results cause errors in product design. Knowledge of material behaviour in various loading conditions is essential to develop accurate material models. Also, heat treatment conditions (Li et al. [15] and Zhong et al. [16]) affect the material properties significantly. Elementary equations for stress calculation need to be modified if there is any crack, notch or hole on the test specimens (Spencer et al. [17] and Moreira et al. [18]). Therefore, in this paper, the tensile behaviour of Al6082-T6 alloy is studied for different strain rates, heat treatment conditions and notches on test specimens with fractography analysis and calibration of existing material models.

2. Experiments

Different test specimens are prepared from the cylindrical rods (12 mm diameter) and flat sheets (6 mm thickness) of Al6082-T6 alloy. The chemical composition (in wt. %) of the alloy is given in Table 1. The alloy has its density 2700 kg/m^3, Vickers hardness 95 HV and thermal conductivity as 180 W/m.K. Gauge sections of the cylindrical specimens have 36 mm length and 9 mm diameter, whereas, gauge sections of the flat specimens have 25 mm length, 6 mm width and 4 mm thickness for tensile tests as per ASTM E8 standard (Fig.1a). Three different notch profiles (C, V and U) are made in flat specimens (Fig.1a). Specimens of C-notches with 3 mm, 4 mm and 5 mm radii; U-notches with 3 mm, 4 mm and 5 mm radii; and V-notches with 60°, 90° and 120° angles; are prepared for investigation.

Table 1

Chemical composition of Al6082-T6 alloy

Elements	Cr	Cu	Fe	Mg	Mn	Si	Ti	Zn	Al
Weight%	0.25	0.10	0.50	1.00	0.80	1.00	0.10	0.20	Balanced

Electromechanical universal testing machine (UTM) of capacity 250 kN from Zwick/Roell, Germany is used for tensile tests (0.0001-0.1s^{-1}) with room

temperature of 25℃. Scanning electron microscope (SEM) is used for fractography analysis of fractured tensile specimens. Muffle furnace (max. 1000℃) is used for heat treatment of unnotched cylindrical specimens at different temperatures (50℃ - 250℃) with heating rate 4℃/min and soaking (holding) time 1-3 hours (h), the specimens are left inside the furnace for slow cooling. Unnotched cylindrical specimens with and without heat treatment are tested under tension (0.0001-0.1s^{-1}) at room temperature to know the effects of heat treatment. Thereafter, notched and unnotched flat specimens are tested at tensile strain rate 0.1s^{-1} to understand the notch sensitivity of the alloy. Experiments conducted on the UTM are controlled with the help of testXpert software. The obtained engineering stress (σ_E) and engineering strain (ε_E) data are converted into true stress (σ_T) and true strain (ε_T) values using equations (1) and (2) respectively.

$$\text{True Stress: } \sigma_T = \sigma_E(1 + \varepsilon_E) \quad (1)$$

$$\text{True Strain: } \varepsilon_T = ln(1 + \varepsilon_E) \quad (2)$$

Fig. 1 Tensile tests (a) unnotched and notched specimens and (b) specimens connected between machine crossheads.

3. Results and Discussion

Tensile tests data are analyzed and the results obtained are discussed. Each data point represents the average of at least three test results. Stress-strain curves (0.0001-0.1s^{-1}) are compared at 25℃ in Fig. 2 and the tensile properties are presented in Table 2. It is found that the alloy is positive strain rate sensitive as the flow stress increases with increasing strain rate. Chen et al. [19] observed similar behaviour (positive sensitive) of the AA6082-T6 alloy at 0.001-1s^{-1} and its insensitivity at 800-3400s^{-1}. For 0.0001s^{-1} to 0.1s^{-1} increased rate, the engineering and true yield strengths (YSs, at 0.2% offset strain) are increased by 19.68% and 20.26% respectively, while the corresponding ultimate tensile strengths (UTSs) are increased by 18.07% and 19.16% respectively. Uniform strain increases while

ductility decreases. Toughness/energy dissipation (area under engineering stress-strain curve) of the alloy increases upto $0.01s^{-1}$ and then decreases at $0.1s^{-1}$. The broken specimens in Fig. 3 shows shear fracture of the material at different strain rates ($0.0001\text{-}0.1s^{-1}$). SEM images (magnification 2000x) are shown in Fig. 4 to study the nature of fracture surfaces. Shallow and depth dimples indicate a typical nucleation-growth-coalescence process of ductile fracture. Size of dimples increases with increasing strain rate ($0.0001\text{-}0.1s^{-1}$). Toric et al. [20] found decreased flow stress of EN 6082AW T6 on increasing temperature (20-350°C) and abnormal behaviour for ductility, i.e., the elongation increased from 20°C to 150°C and then decreased upto 300°C and again increased at 350°C. Also, Torca et al. [21] observed reduced strength and improved elongation of 6082-T6 with increasing temperature (25-250°C) and found lower elongation at 250°C compared to that at 25°C.

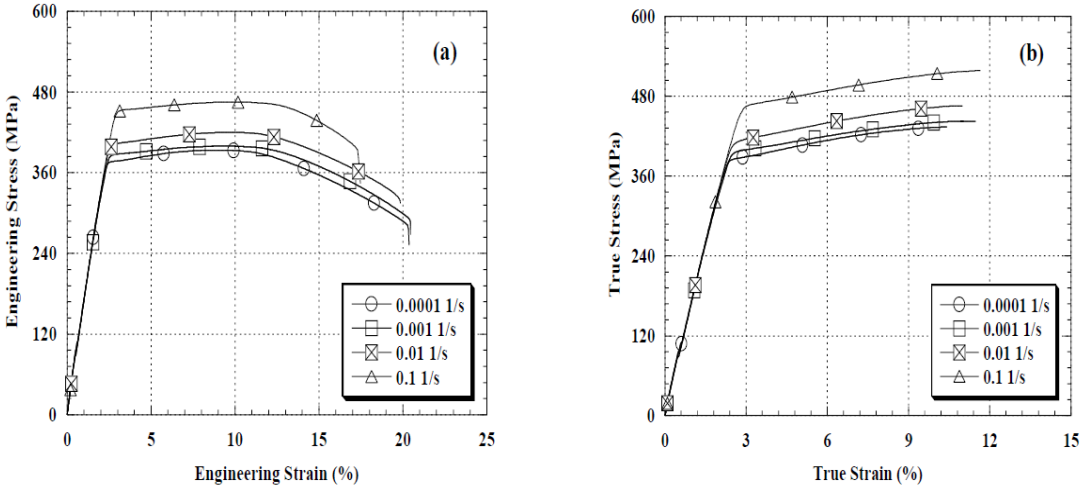

Fig. 2 Stress-strain curves at $0.0001\text{-}0.1s^{-1}$.

Table 2

Tensile test results of Al6082-T6 for unnotched specimens at room temperature

Strain Rate (s^{-1})	Engineering stress-strain curves				Toughness (Area under engineering stress-strain curve) (MJ/m^3)	True stress-strain curves	
	YS (MPa)	UTS (MPa)	Uniform Strain (%)	Total Elongation (%)		YS (MPa)	UTS (MPa)
0.0001	371 ± 3	393 ± 3	1.26 ± 0.01	20 ± 0.4	70 ± 1.5	380 ± 3	428 ± 3
0.001	381 ± 3	399 ± 3	2.14 ± 0.02	20 ± 0.5	72 ± 1	391 ± 3	436 ± 4
0.01	396 ± 3	419 ± 4	2.52 ± 0.03	19.5 ± 0.4	74 ± 2	406 ± 4	460 ± 4
0.1	444 ± 4	464 ± 5	2.62 ± 0.03	17.5 ± 0.3	72 ± 1	457 ± 4	510 ± 5

Fig. 3 Broken tensile specimens.

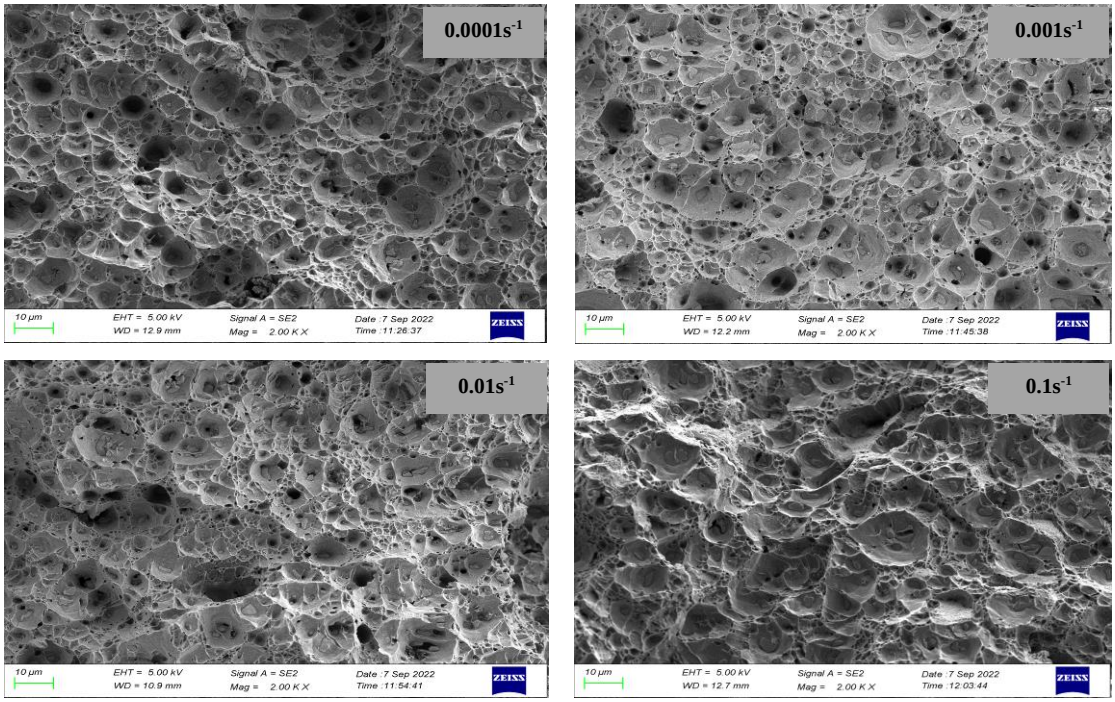

Fig. 4 SEM images of fractured surfaces at different strain rates.

3.1 Effects of Heat Treatment

Experiments are carried out for heat-treated (50℃, 150℃ and 250℃; heating rate 4℃/min, soaking time 1-3 h) cylindrical specimens under tension ($0.1s^{-1}$) and the obtained stress-strain curves are compared as shown in Fig. 5. Tensile properties of the alloy for heat-treated specimens are tabulated in Table 3. It is found that the strength of the alloy decreases and ductility increases with heat treatment. After heat treatment at 50℃, 150℃ and 250℃, the true YSs of the alloy are decreased by 9.40%, 18.16% and 48.58% respectively, whereas, the corresponding true UTSs are decreased by 7.84%, 15.68% and 33.53% respectively. On increasing temperature from 50℃ to 250℃ for constant soaking (holding) time 1 h, the YSs are decreased by 42.43% (engineering) and 43.24% (true) whereas, the UTSs are decreased by 28.34% (engineering) and 27.87%

(true). On increasing soaking time from 1 h to 3 h at constant temperature, the YSs are increased by 7.38% (engineering) and 7.75% (true), whereas, the UTSs are increased by 7.12% (engineering) and 7.91% (true) due to precipitation strengthening process. Mrówka-Nowotnik et al. [22] found the similar results and concluded that the crack resistance and critical fracture toughness factor of the alloy are strongly influenced by the heat treatment process. Wang et al. [23] found increased amount of precipitates and diminished work hardening on increased annealing temperature. The morphology (Fig. 6) of the fractured specimens shows shear fracture of the alloy. Shallow and depth dimples are found. However, after heat treatment, more deeper dimples are observed as compared to the fractured specimens at room temperature (25°C). For increased holding time at constant temperature, size of dimples increases.

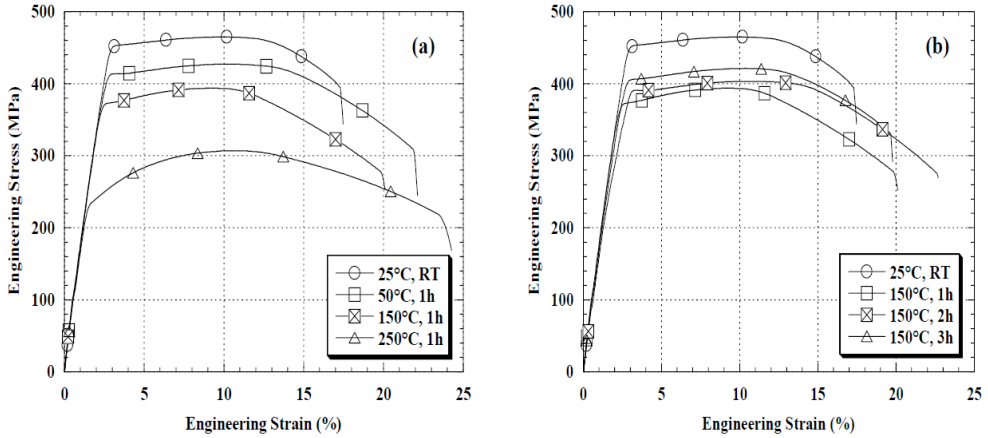

Fig. 5 Comparison of stress-strain curves for heat-treated cylindrical specimens.

Table 3

Tensile test results of Al6082-T6 for unnotched heat-treated specimens at 0.1s^{-1}

Heat Treatment Temperature (°C)	Soaking Time (Hour)	Engineering stress-strain curves				Toughness (Area under engineering stress-strain curve) (MJ/m^3)	True stress-strain curves	
		YS (MPa)	UTS (MPa)	Uniform Strain (%)	Total Elongation (%)		YS (MPa)	UTS (MPa)
50	1	403 ± 4	427 ± 4	1.95 ± 0.02	22 ± 0.3	77 ± 2	414 ± 4	470 ± 5
150	1	366 ± 3	393 ± 3	1.55 ± 0.02	20 ± 0.2	64 ± 1.5	374 ± 3	430 ± 3
250	1	232 ± 2	306 ± 3	1.02 ± 0.01	24 ± 0.3	63 ± 1	235 ± 3	339 ± 3
150	2	376 ± 3	403 ± 3	1.12 ± 0.01	22.5 ± 0.2	74 ± 2	386 ± 3	446 ± 4
150	3	393 ± 3	421 ± 4	0.62 ± 0.01	20 ± 0.3	68 ± 1.5	403 ± 4	464 ± 5

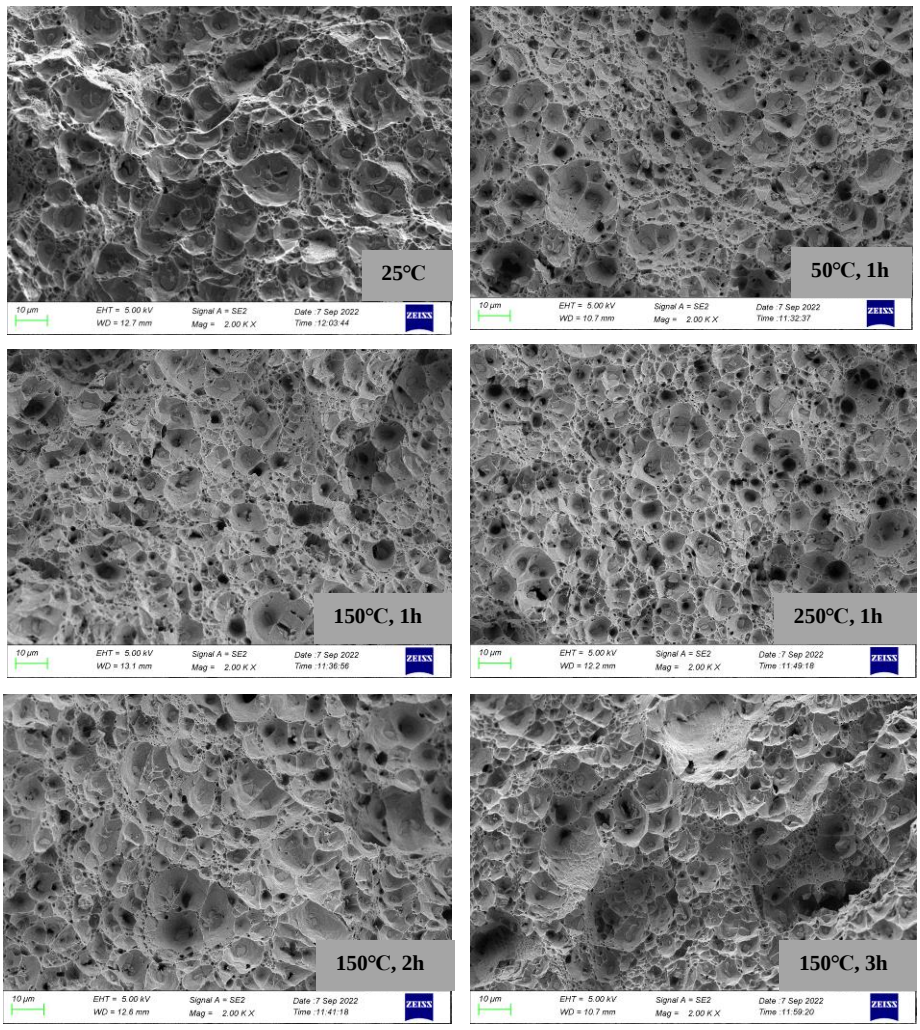

Fig. 6 Fractographs of heat-treated and non-heat-treated broken specimens.

3.2 Effects of Notch profiles

Stress-strain curves of the Al6082-T6 alloy for different notched (C, U and V) specimens are compared with that of unnotched specimen under tension ($0.1s^{-1}$) in Fig. 7. Tensile properties for various notch profiles are given in Table 4. The alloy has smooth yielding and due to stress concentration at notches, strengths and plastic deformation of notched specimens decreased as compared to the unnotched specimen. For notched specimens, on increasing notch radius/angle, the YS and UTS of the alloy decrease. Uniform strain, total elongation and toughness (energy dissipation) are slightly higher for C and U notched specimens compared to the V notched specimen, whereas, the alloy shows its higher strength (YS and UTS) for

V notched specimen compared to the C and U notched specimens. For C-notched specimens, on increasing notch radius from 3 mm to 5 mm, the YSs are decreased by 2.23% (engineering) and 2.46% (true), whereas, the corresponding UTSs are decreased by 1.74% and 2.26% respectively. For U-notched specimens, on increasing notch radius from 3 mm to 5 mm, the YSs are decreased by 2.56% (engineering) and 3.45% (true), whereas, the corresponding UTSs are decreased by 2.40% and 2.24% respectively. For V-notched specimens, on increasing notch angle from 60° to 120°, the YSs are decreased by 5.50% (engineering) and 6.31% (true), whereas, the corresponding UTSs are decreased by 4.88% and 5.59% respectively. Among C-, U- and V-notched specimens, the V-notched specimen can sustain more load at all angles, 60°-120° and dissipate less energy because of comparatively reduced deformation. The U-notched specimens show better alloy strength as compared to C-notched specimens. Fig. 7d shows that all the specimens have ductile fracture at their notches due to stress concentration.

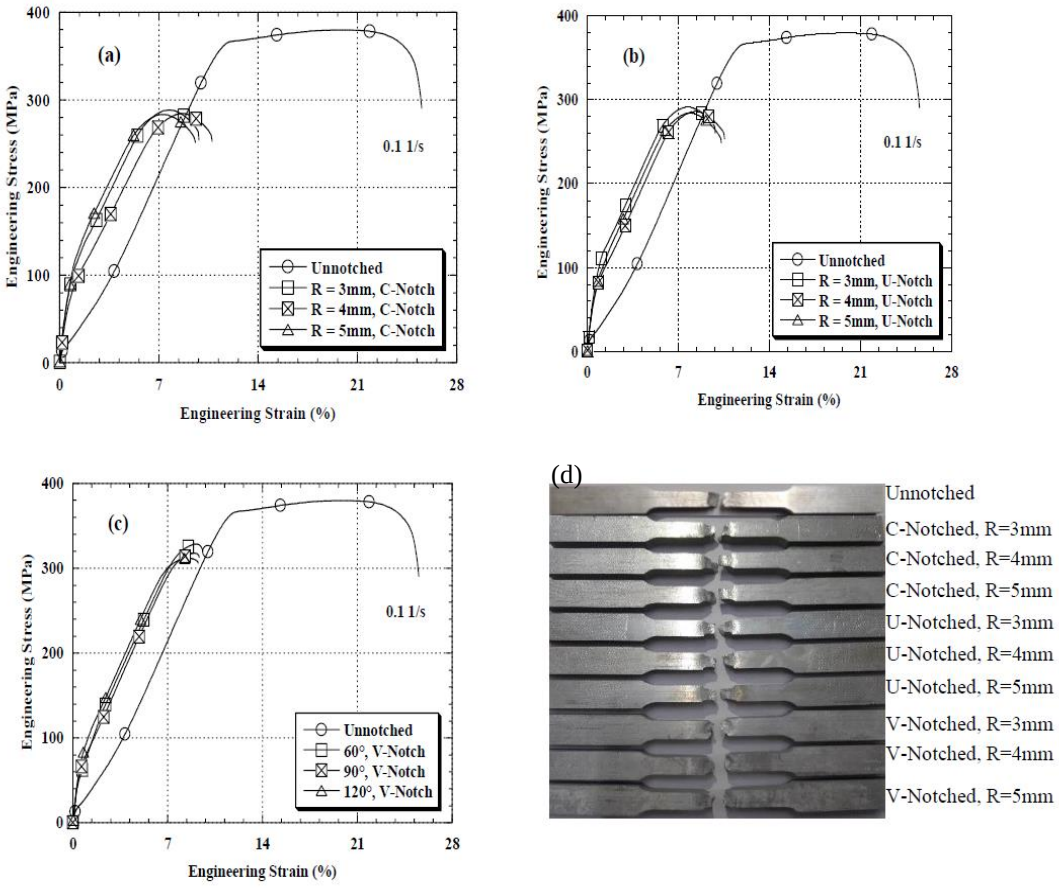

Fig. 7 Stress-strain curves for notched and unnotched specimens with their broken pieces.

Table 4

Tensile properties of Al6082-T6 for notched specimens at $0.1s^{-1}$

Notch Profiles	Notch Radius (mm)/ Angle (°)	Engineering stress-strain curves				Toughness (Area under engineering stress-strain curve) (MJ/m^3)	True stress-strain curves	
		YS (MPa)	UTS (MPa)	Uniform Strain (%)	Total Elongation (%)		YS (MPa)	UTS (MPa)
C	R = 3mm	269 ± 2	288 ± 3	0.58 ± 0.006	10 ± 0.15	17.5 ± 0.3	285 ± 3	310 ± 3
	R = 4mm	264 ± 2	284 ± 3	0.70 ± 0.007	10.7 ± 0.1	18.5 ± 0.3	280 ± 3	309 ± 3
	R = 5mm	263 ± 2	283 ± 2	0.61 ± 0.006	9.5 ± 0.1	17.5 ± 0.3	278 ± 2	303 ± 3
U	R = 3mm	273 ± 3	291 ± 3	0.53 ± 0.005	10 ± 0.15	18 ± 0.3	290 ± 3	313 ± 4
	R = 4mm	269 ± 2	286 ± 3	0.77 ± 0.008	10.5 ± 0.1	18 ± 0.3	283 ± 3	309 ± 3
	R = 5mm	266 ± 2	284 ± 2	0.52 ± 0.005	10.3 ± 0.1	18.5 ± 0.3	280 ± 2	306 ± 3
V	θ = 60°	309 ± 3	328 ± 4	0.26 ± 0.003	9.5 ± 0.1	16.5 ± 0.2	333 ± 4	358 ± 4
	θ = 90°	299 ± 2	318 ± 3	0.30 ± 0.003	9.3 ± 0.1	15.5 ± 0.15	321 ± 3	346 ± 4
	θ = 120°	292 ± 2	312 ± 3	0.70 ± 0.007	9.2 ± 0.1	16 ± 0.25	312 ± 3	338 ± 3
Unnotched	R = 0	356 ± 3	379 ± 4	2.59 ± 0.026	25.5 ± 0.5	65 ± 1	396 ± 4	455 ± 5

3.3 Material models

The Cowper-Symonds (CS) and Johnson-Cook (JC) models for Al6082-T6 alloy are evaluated based on the experimental data (untreated cylindrical specimens) using curve fitting method. The material constants (D and q) are determined in Fig. 8a and the well fitted CS model is given in equation (3). The predicted results of the CS model have good agreement with the experimental results in Fig. 8b.

$$\sigma_{CS} = (380) \times \left[1 + \left(\frac{\dot{\varepsilon}}{4.6497}\right)^{\frac{1}{2.356}}\right] \tag{3}$$

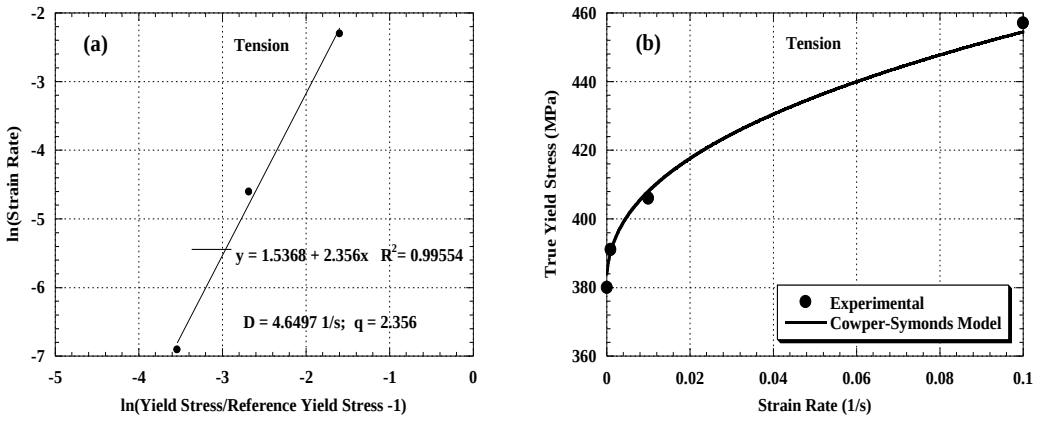

Fig. 8 CS model (a) calculation of material parameters and (b) agreement of the predicted results with the experimental results.

The Cowper-Symonds model is used when only strain rate effects are to be checked, whereas, the Johnson-Cook model is suitable when strain rate hardening, strain rate sensitivity and temperature effects are to be monitored for materials. The JC model for the alloy can be represented by equation (4) [24]**;**

$$\sigma_{JC} = \left(A + B\varepsilon_p^n\right) \times \left(1 + C \ln \dot{\varepsilon}^*\right) \tag{4}$$

In this paper, thermal effect is not incorporated in the JC model. The material constants of this model are, $A = 380$ MPa, $B = 1735.2$ MPa, $n = 1.4242$ and, C at $0.001s^{-1}$, $0.01s^{-1}$ and $0.1s^{-1}$ are 0.0074121, 0.013783 and 0.026409 respectively. Here, σ_{JC} is the true stress, ε_p is the true plastic strain, $\dot{\varepsilon}^* = \frac{\dot{\varepsilon}}{\dot{\varepsilon_0}}$ where $\dot{\varepsilon_0} = 0.0001s^{-1}$. The predicted results of the JC model are matched with the experimental results in Fig. 9.

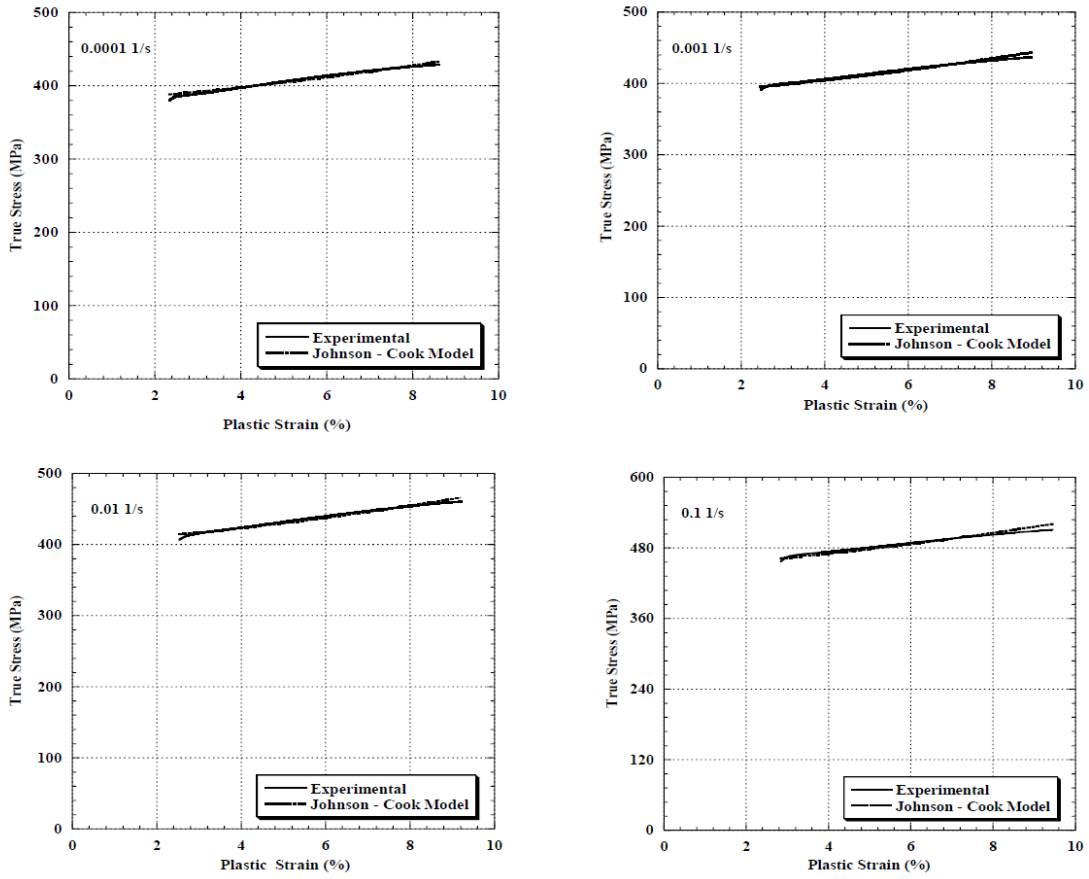

Fig. 9 Agreement of the predicted results by JC model with the experimental results.

4. Conclusions

Following conclusions are drawn from the present investigation:

- The Al6082-T6 aluminium alloy is positive strain rate sensitive under tension ($0.0001\text{-}0.1s^{-1}$) at room temperature 25℃. Energy dissipation of the alloy is nearly 70-74 MJ/m^3 for non-heat-treated specimens.
- The alloy shows good ductility at $0.0001\text{-}0.1s^{-1}$ as the elongation in stress-strain curve is around 17-20% and the uniform strain increases with increasing strain rate. The alloy has ductile fracture.
- The heat treatment conditions (soaking time and temperature) affect the tensile properties of the alloy. Heat treatment (50-250℃) reduces the alloy strength and increases its ductility.
- The alloy is notch sensitive i.e, the tensile properties depend on different notch profiles (C, U and V) and their dimensions. On increasing notch radius/angle, the YS and UTS of the alloy decrease.
- The estimated CS and JC models represent the flow stress of the alloy very well.

R E F E R E N C E S

[1]. *D-N Zhang, Q-Q Shangguan, C-J Xie and F. Liu,* "A modified Johnson–Cook model of dynamic tensile behaviors for 7075-T6 aluminum alloy", Journal of Alloys and Compounds, 619, 2015, 186-194.

[2]. *R. Branco, J.D. Costa, L.P. Borrego, S.C. Wu, X.Y. Long and F.V. Antunes,* "Effect of tensile pre-strain on low-cycle fatigue behaviour of 7050-T6 aluminium alloy", Engineering Failure Analysis, 114, 2020, 104592.

[3]. *G. Prakash, N.K. Singh and N.K. Gupta,* "Deformation behaviours of Al2014-T6 at different strain rates and temperatures", Structures, 26, 2020, 193-203.

[4]. *G. Prakash, N.K. Singh, P. Sharma and N.K. Gupta,* "Tensile, compressive, and flexural behaviors of Al5052-H32 in a wide range of strain rates and temperatures", Journal of Materials in Civil Engineering, 32(5), 2020, 04020090.

[5]. *H. Deng, S. Yang, G. Li, X. Zhang and J. Cui,* "Novel method for testing the high strain rate tensile behavior of aluminum alloys", Journal of Materials Processing Tech. 280, 2020, 116601.

[6]. *J.Q. Tan, M. Zhan, S. Liu, T. Huang, J. Guo and H. Yang, "*A modified Johnson–Cook model for tensile flow behaviors of 7050-T7451 aluminum alloy at high strain rates", Materials Science and Engineering: A, 631, 2015, 214-219.

[7]. *X. Wang, X. Fan, X. Chen and S. Yuan,* "Cryogenic deformation behavior of 6061 aluminum alloy tube under biaxial tension condition", Journal of Materials Processing Technology, 303, 2022, 117532.

[8]. *R. Tandon, K. K. Mehta, R. Manna and R. K. Mandal, "*Effect of tensile straining on the precipitation and dislocation behavior of AA7075T7352 aluminum alloy", Journal of Alloys and Compounds, 904, 2022, 163942.

[9]. *R. Bobbili, V. Madhu and A. K. Gogia,* "Tensile behaviour of aluminium 7017 alloy at various temperatures and strain rates", Journal of Materials Research and Technology, 5 (2), 2016, 190-197.

[10]. *S. Hashemian, P. M. Keshtiban and A. E. Oskui,* "Fracture behavior of the forged aluminum 7075-T6 alloy under mixed-mode loading conditions", Engineering Failure Analysis, 140, 2022, 106610.

[11]. *K. Huang, S. Huang, Y. Yi, F. Dong and H. He,* "Flow behavior and forming characteristics of 2A14 aluminum alloy at cryogenic temperatures", Journal of Alloys and Compounds, 902, 2022, 163821.

[12]. *Ł. Derpeński, A. Seweryn and J. Bartoszewicz, "*Ductile fracture of notched aluminum alloy specimens under elevated temperature part 1 – Experimental research", Theoretical and Applied Fracture Mechanics, 102, 2019, 70-82.

[13]. *E. Combaz, A. Rossoll and A. Mortensen,* "Hole and notch sensitivity of aluminium replicated foam", Acta Materialia, 59 (2), 2011, 572-581.

[14]. *C. Mondal, B. Mishra, P. K. Jena, K. S. Kumar and T. B. Bhat,* "Effect of heat treatment on the behavior of an AA7055 aluminum alloy during ballistic impact", International Journal of Impact Engineering, 38 (8–9), 2011, 745-754.

[15]. *B. Li, X. Wang, H. Chen, J. Hu, C. Huang and G. Gou,* "Influence of heat treatment on the strength and fracture toughness of 7N01 aluminum alloy", Journal of Alloys and Compounds, 678, 2016, 160-166.

[16]. *H. Zhong, P. Rometsch and Y. Estrin,* "Effect of alloy composition and heat treatment on mechanical performance of 6xxx aluminum alloys", Transactions of Nonferrous Metals Society of China, 24 (7), 2014, 2174-2178.

[17]. *K. Spencer, S. F. Corbin and D. J. Lloyd,* "Notch fracture behaviour of 5754 automotive aluminium alloys", Materials Science and Engineering: A, 332 (1–2), 2002, 81-90.

[18]. *P. M. G. P. Moreira, F. M. F. D. Oliveira and P. M. S. T. D. Castro,* "Fatigue behaviour of notched specimens of friction stir welded aluminium alloy 6063-T6", Journal of Materials Processing Technology, 207 (1–3), 2008, 283-292.

[19]. *X. Chen, Y. Peng, S. Peng, S. Yao, C. Chen and P. Xu,* "Flow and fracture behavior of aluminum alloy 6082-T6 at different tensile strain rates and triaxialities", PLOS ONE, 12(7), e0181983; https://doi.org/10.1371/journal.pone.0181983.*I.*

[20]. *N. Torić, J. Brnić, I. Boko, M. Brčić, I. W. Burgess and I. Uzelac,* "Experimental Analysis of the Behaviour of Aluminium Alloy EN 6082AW T6 at High Temperature", Metals, 7, 126, 2017, 1-15; doi:10.3390/met7040126.

[21]. *Torca, A. Aginagalde, J.A. Esnaola, L. Galdos, Z. Azpilgain and C. Garcia,* Tensile behaviour of 6082 aluminium alloy sheet under different conditions of heat treatment, temperature and strain rate", Key Engineering Materials, 423, 2010, 105-112.

[22]. *G. Mrówka-Nowotnik, J. Sieniawski and A. Nowotnik,* "Tensile properties and fracture toughness of heat treated 6082 alloy", Journal of Achievements in Materials and Manufacturing Engineering, 17 (1-2), 2006, 105-108.

[23]. *B. Wang, X-H. Chen, F-S. Pan, J-J. Mao and Y. Fang,* "Effects of cold rolling and heat treatment on microstructure and mechanical properties of AA 5052 aluminum alloy", Transactions of Nonferrous Metals Society of China, 25 (8), 2015, 2481-2489.

[24] *N.K. Singh, E. Cadoni, M.K. Singha and N.K. Gupta,* "Dynamic Tensile and Compressive Behaviors of Mild Steel at Wide Range of Strain Rates", J. Eng. Mech., 139(9), 2013, 1197-1206.